# Nanoscale

Accepted Manuscript


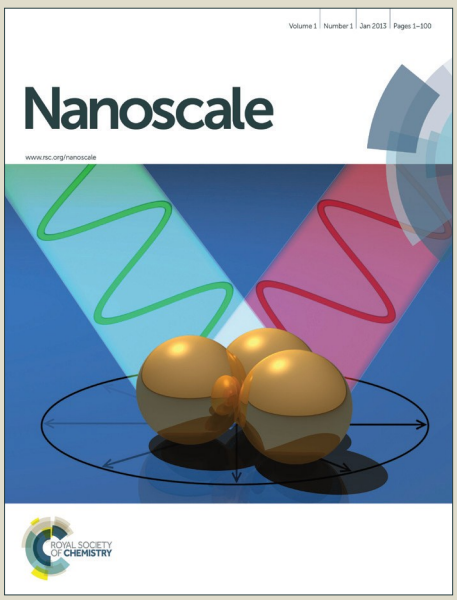





ROYAL SOCIETY OF CHEMISTRY

www.rsc.org/nanoscale

Journal Name

ARTICLE

# Investigation of the mimetic enzyme activity of two-dimensional Pd-based nanostructures

Received 00th January 20xx,
Accepted 00th January 20xx

DOI: 10.1039/x0xx00000x

www.rsc.org/

Jingping Wei, Xiaolan Chen,* Saige Shi, Shiguang Mo and Nanfeng Zheng*

In this work, we investigated the mimetic enzyme activity of two-dimensional (2D) Pd-based nanostructures (e.g. Pd nanosheets, Pd@Au and Pd@Pt nanoplates) and found they possessed intrinsic peroxidase-, oxidase- and catalase-like activity. These nanostructures were able to activate hydrogen peroxide or dissolved oxygen for catalyzing the oxidation of organic substrates, and decompose hydrogen peroxide to generate oxygen. More systematic investigations revealed that the peroxidase-like activities of these Pd-based nanomaterials were highly structure- and composition- dependent. Among them, Pd@Pt nanoplates displayed the highest peroxidase-like activity. Based on these findings, Pd-based nanostructures were applied for the colorimetric detection of $H_2O_2$ and glucose, and also the electro-catalytic reduction of $H_2O_2$. This work offers a promising prospect for the application of 2D noble metal nanostructures in biocatalysis.

## 1 Introduction

Natural enzymes have been widely used in the fields of industry, agriculture, medicine, hygiene and foods because of their high specificity and catalytic efficiency under mild reaction conditions.[1] However, they have some shortcomings such as low stability, and high costs in preparation and purification, and high sensitivity of catalytic activity to environments.[2] Therefore, the use of mimetic enzyme substitutes for natural enzyme has markedly increased in recent years.

To date, many organic molecules, polymers, biomolecules and nanoparticles (NPs) have been developed as effective mimic enzymes exhibiting peroxidase-, oxidase- or catalase-like activity.[3-37] Among them, metallic NPs, especially noble metal NPs, have attracted great interests due to their unique optical, electronic and catalytic properties.[16-37] These properties are closely related to their size, shape, structure and composition.[38-40] For example, small Pt NPs were suggested to act as a potent SOD/catalase mimics as they could effectively scavenge superoxide free radicals and $H_2O_2$.[16, 17] Au NPs with different surface modifications have been reported to demonstrate different enzyme-like activity.[19-21] By forming appropriate bimetallic composite nanostructures, such as AgM (M=Au, Pd, Pt) nanoalloys,[22] Au@Pt core-shell nanorods[23, 24] and PdPt nanodots on gold nanorods,[25] the peroxidase- or oxidase-like catalytic activities can be well tuned via varying alloy composition. Also, enhanced catalytic performances have been widely observed by loading noble metal NPs on various supports (e.g. graphene, $MoO_3$ and $Fe_3O_4$, etc) because of their synergistic effect.[26-31]

Although important progress has been achieved for the study of noble metal-based enzyme-like catalysts, there are rare reports on the enzyme mimic application of their two-dimensional (2D) nanostructures. Recently, 2D hexagonal palladium nanosheets (Pd NSs) with well-defined thickness and sizes have been successfully synthesized by our group[41] and applied in catalysis, cancer diagnosis and treatment,[42-46] because of their strong near-infrared surface plasma resonance (SPR) properties, high photothermal conversion efficiency, and excellent biocompatibility. Moreover, other noble metals, such as Au and Ag, were readily grown on the surface of Pd NSs[47-50] to prepare core-shell noble metal nanoplates, which also displayed excellent photothermal properties[50] and bactericidal activity.[51]

In this work, we found that several 2D Pd-based nanostructures (Pd NSs, Pd@Au and Pd@Pt nanoplates) possessed intrinsic peroxidase-, oxidase- and catalase-like activity. These nanostructures readily catalyzed hydrogen peroxide and oxygen reduction and the dismutation decomposition of hydrogen peroxide to generate oxygen. We focused the investigation on their peroxidase-like activity and

*State Key Laboratory for Physical Chemistry of Solid Surfaces, Collaborative Innovation Center of Chemistry for Energy Materials, and Engineering Research Center for Nano-Preparation Technology of Fujian Province, College of Chemistry and Chemical Engineering, Xiamen University, Xiamen 361005, China.*
*E-mail: chenxl@xmu.edu.cn; nfzheng@xmu.edu.cn.*

† Electronic Supplementary Information (ESI) available: [TEM images, EDX and dispersion stability of Pd-based nanomaterials, mimic enzymatic activity and reaction mechanism for TMB oxidation with $H_2O_2$ catalyzed by Pd-based nanoplates, time-dependent absorbance changes at 652 nm with different $H_2O_2$ concentrations, comparison of peroxidase activity of Pd@Pt-a (Pt/Pd=1.3) and Pd@Pt-e (Pt/Pd=12) with their corresponding monometallic components, reaction between hydroxyl radical (•OH) and terephthalic acid (TA), comparison of the peroxidase- and oxidase- like activities of Pd@Pt before and after centrifugation, relative catalytic activity of the Pd@Pt nanoplates after incubation at a range of values of pH, temperatures or storing in water for one week, UV-Vis absorption spectra of TMB under different conditions, steady-state kinetic assay of Pd and catalytic mechanism of Pd@Pt, detailed calculating process for *Km* and *Vmax*, and experimental condition optimization of Pd@Pt peroxidase-like catalytic reaction]. See DOI: 10.1039/x0xx00000x.

found that Pd NSs coated with a shell composed of Pt nanodots (Pd@Pt nanoplates) demonstrated higher mimic enzyme activity than Pd NSs, whereas Pd@Au nanoplates, in which Au was epitaxially grown on Pd NSs, have lower catalytic activity than Pd NSs. Besides the influence of structures, the enzyme-like activities can be easily tuned by tailoring the composition of Pd and Au (or Pt). On basis of these findings, the outstanding peroxide-like activity of Pd@Pt nanoplates was then applied to the colorimetric detection of $H_2O_2$ and glucose. Moreover, the electrochemical $H_2O_2$ analysis was also demonstrated based on the electrocatalytic activity of Pd-based nanostructures.

## 2 Experimental Section

### Materials

$Pd(acac)_2$, $Pt(acac)_2$, $AuPPh_3Cl$ and 3,3',5,5'-tetramethylbenzidine (TMB) were purchased from Sigma-Aldrich. PVP (MW=30000), N, N-dimethylformamide (DMF), tetrabutylammonium bromide (TBAB) and hydrogen peroxide ($H_2O_2$) (30%) were the products of Sinopharm Chemical Reagent Co. Ltd. (Shanghai, China). The water used in all experiments was ultrapure (18.2 MΩ). All reagents were used as received without further purification.

### Characterization

TEM studies were performed on JEM 1400 transmission electron microscope and TECNAI F-30 high-resolution transmission electron microscope operating at 300 kV. Absorption measurements were carried out on a UV2550 spectrophotometer (Shimadzu) or Cary 5000 UV-Vis-NIR spectrophotometer (Varian). The electrochemical $H_2O_2$ analysis was performed using an electrochemical work station (CHI760E).

### Preparation of Pd nanosheets (Pd NSs)

Pd NSs were prepared according to our previously reported method.[41] In brief, $Pd(acac)_2$ (50.0 mg), PVP (160.0 mg) and TBAB (160 mg) were mixed together with DMF (10.0 mL) and water (2.0 mL) in a glass pressure vessel. The vessel was then charged with CO to 1 bar and heated from room temperature to 90 °C in 1 h, and then kept at 90 °C for another 3 h before being cooled to room temperature. The obtained dark blue products were precipitated by acetone, and purified by an ethanol–acetone mixture for further use.

### Preparation of Pd@Au and Pd@Pt bimetallic nanoplates

To prepare Pd@Au bimetallic nanoplates with different Au/Pd ratios, 0.1 mL above synthesized Pd NSs stock solution (1.2 mg $mL^{-1}$) and different mass (e.g. 0.5, 1, 2, 3.5 and 5 mg) of $AuPPh_3Cl$ (2 mg $mL^{-1}$ in DMF) were mixed in DMF, respectively. Then hydrazine (80%, 100 μL) was added dropwise while the mixture was stirred vigorously. After all the above were done, the solution was left undisturbed at room temperature for more than 12 h. The products were precipitated by acetone, separated via centrifugation, and further purified by an ethanol–acetone mixture. The resulting solution was stored at 4 °C for future use.

In the case of Pd@Pt bimetallic nanoplates with different Pt/Pd ratios, the similar procedure was applied except that different mass of $Pt(acac)_2$ (2 mg $mL^{-1}$ in DMF) was used to replace $AuPPh_3Cl$ and the solution was left undisturbed at 100 °C for more than 12 h.

The amounts of Pd, Au and Pt were also measured by ICP-MS (the mass ratios of Au/Pd from a to e are 1.5:1, 2.4:1, 3.2:1, 7.0:1 and 8.2:1 respectively; the mass ratios of Pt/Pd from a to e are 1.3:1, 2.9:1, 5:1, 8:1 and 12:1, respectively).

### Mimic enzymatic activity of Pd-based nanoplates

In order to investigate mimic enzymatic activity of Pd-based nanoplates, time-dependent absorbance changes at 652 nm and absorbance spectra of 0.25 mM TMB solutions containing 5 mM $H_2O_2$ or dissolved $O_2$ with Pd-based nanoplates were measured and photographed respectively. The catalase-like activity of Pd-based nanoplates and catalase was compared with a pen-like pressure meter.[52] The pressure values were measured in a closed rubber covered 96-well plate system containing $H_2O_2$ with different catalysts.

### Experimental condition optimization

The catalytic activity of the Pd-based nanoplates is dependent on pH, temperature, the concentration of catalyst, and $H_2O_2$ concentrations. In the work, Pd@Pt nanoplates were chosen as the model catalysts to study the catalytic activity in different experimental conditions. (Detailed experimental procedures were demonstrated in Supporting Information).

### Comparing the peroxidase-like activity of Pd, Pd@Au, Pd@Pt and Pt nanoparticles

Similar to peroxidase, Pd-based nanoplates can catalyze the reaction of the substrate 3,3',5,5'-tetramethylbenzidine (TMB) by $H_2O_2$ to produce a blue color product, with maximum absorbance at 652 nm. To study the peroxidase-like activity of Pd, Pd@Au and Pd@Pt with different ratios, time-dependent absorbance changes at 652 nm and UV-Vis spectra were performed in a reaction volume of 2 mL buffer solution (acetic acid-sodium acetate buffer solution, pH 4.5) with 0.5 mM TMB and 10 mM $H_2O_2$ using Pd, Pd@Au or Pd@Pt as catalysts, respectively. To compare the catalytic activity of Pd@Pt and its components, 0.5 mM TMB and 10 mM $H_2O_2$ in 2 mL buffer solution (pH=4.5) were measured with four different catalysts: (1) Pd@Pt-c (containing 0.03 μg Pd NSs and 0.15 μg Pt nanodots), (2) physical mixture of 0.03 μg Pd NSs and 0.15 μg Pt nanoparticles (NPs), (3) only 0.03 μg Pd NSs and (4) only 0.15 μg Pt NPs. The same experimental process was used to compare the peroxidase-like activity of Pd@Pt with other ratios.

### Kinetic studies of the peroxidase-like activity of Pd and Pd@Pt nanoplates

Kinetic measurements were carried out in time-drive mode by monitoring the absorbance change at 652 nm on a UV-Vis

spectrophotometer. To investigate the mechanism, assays were carried out by varying concentrations of TMB at a fixed concentration of $H_2O_2$ or vice versa. The Michaelis-Menten constant was calculated using Lineweaver-Burk plots of the double reciprocal of the Michaelis-Menten equation: $1/V = (K_m/V_{max})\cdot(1/[S] + 1/K_m)$, where $V$ is the initial velocity, $V_{max}$ is the maximal reaction velocity, $[S]$ is the concentration of substrate, $K_m$ is the Michaelis constant and $K_m$ approximates the affinity of the enzyme for the substrate.

**Colorimetric detection of $H_2O_2$ and Glucose**

To a 2 mL HAc-NaAc buffer solution (pH=4.5) containing 0.5 mM TMB and 0.65 μg Pd@Pt, different concentrations of $H_2O_2$ were added respectively. The mixed solution was used to measure the UV absorption at the wavelength of 652 nm.

Glucose detection procedure was shown as follows: (1) 100 μL of 2 mg $mL^{-1}$ GOx and 100 μL of glucose with different concentration in PBS buffer solution (pH 7.4) were incubated at 37 °C for 2 h; (2) the above glucose reaction solutions were added into 2 mL acetic acid-sodium acetate buffer solution (pH 4.5) containing 0.5 mM TMB and 0.65 μg Pd@Pt. The mixed solution was used to perform the measurement.

**Electrochemical $H_2O_2$ analysis**

The electrochemical voltammetric measurements are performed on an electrochemical analysis station (CHI 760e), which is connected to a personal computer. Electrocatalytic activity was tested by measuring the response current of the Pd, Pd@Pt and Pd@Au modified electrodes. The experiment was carried out with a traditional three-electrode cell: a glass carbon (GC) working electrode, an Ag/AgCl reference electrode and a platinum wire electrode. The GC working electrode was polished and further coated with Pd (1 mg $mL^{-1}$, 5 μL), Pd@Pt (1 mg $mL^{-1}$, 5μL) or Pd@Au (1 mg $mL^{-1}$, 5 μL), then 5 μL of Nafion (0.5% in ethanol) was spread on the modified electrodes surface as a binder to hold the film on the electrodes surface stably. The as-prepared electrodes were used separately to detect the $H_2O_2$ with different concentrations (0, 2, 4, 6, 8 and 10 mM) in a 60 mL voltammetric cell with $N_2$-saturated PBS buffer, scanning from -0.6 V to +0.4 V at a scan rate of 50 mV $s^{-1}$. Moreover, the current–time responses of the Pd, Pd@Pt and Pd@Au modified electrodes toward the $H_2O_2$ was carried out with a step of 0.1 mM $H_2O_2$ at an applied potential of -0.2 V

## 3 Results and discussion

**Synthesis and characterization of Pd-based nanoplates**

As shown in Fig.1a, ultrathin hexagonal Pd nanosheets (Pd) with an average edge length of 40 nm were first synthesized according to our previously reported method,[41] and then were used as seeds for the formation of bimetallic Pd@Au or Pd@Pt nanoplates (see the Experimental Section for details). By chemical reducing $AuPPh_3Cl$ or $Pt(acac)_2$ with hydrazine hydrate in the DMF solution, Pd@Au and Pd@Pt nanoplates with different Au/Pd and Pt/Pd mass ratios can be successfully prepared. Au showed an epitaxial growth mode on the Pd NSs, and the cover degree of Au on Pd NSs with different Au/Pd mass ratios had a distinct difference (Fig.1b and 1c). With the lower Au/Pd mass ratio, Au cannot completely cover the surface of Pd NSs and still some palladium are exposed (Fig.1b and Fig.S1). As the increase of gold content, the surface of Pd NSs was increasingly and eventually completely covered to form bimetallic Pd@Au nanoplates (Fig.1c). While the Pt presents an island growth mode on the Pd NSs, and the content and size of Pt nanodots enhance with the increase of Pt/Pd ratios (Fig.1d, 1e and Fig.S2). Furthermore, the obtained Pd@Au and Pd@Pt nanoplates still kept a hexagonal shape and had a mean side length 40 nm, similar to the Pd seeds (Fig.1a). The prepared Pd, Pd@Au and Pd@Pt exhibited good

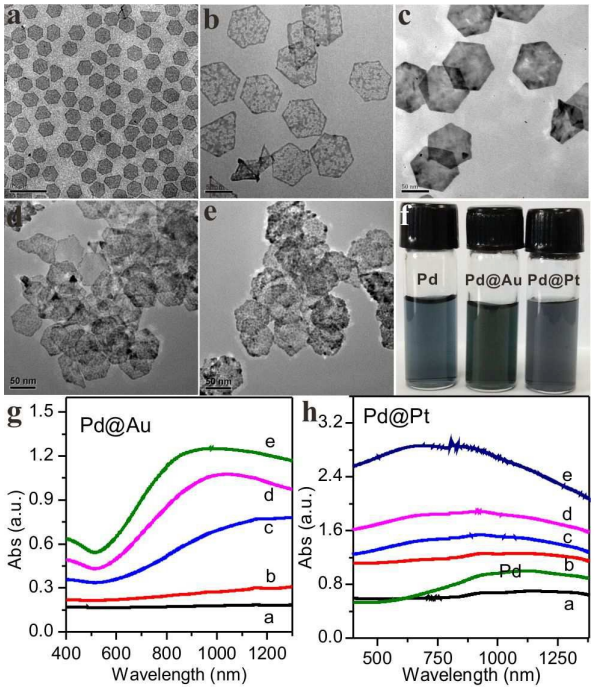


**Fig.1** Representative TEM images of Pd NSs (a), Pd@Au nanoplates with the mass ratios of Au/Pd 1.5:1 (b) and 8.2:1 (c), Pd@Pt nanoplates with the mass ratios of Pt/Pd 5.0:1 (d) and 12:1 (e). (f) Photographs of the synthesized Pd NSs, Pd@Au and Pd@Pt nanoplates in water. UV-Vis-NIR absorption spectra of Pd@Au (g) and Pd@Pt (h) nanoplates with different ratios (The mass ratios of Au/Pd from a to e: 1.5:1, 2.4:1, 3.2:1, 7.0:1 and 8.2:1 respectively, and the mass ratios of Pt/Pd from a to e: 1.3:1, 2.9:1, 5:1, 8:1 and 12:1 respectively). The amounts of Pd, Au and Pt were measured by ICP-MS).

dispersion stability in aqueous solution (Fig.1f). When these nanostructures are stored in water for 1 week, no significant decrease of absorption intensity has been observed (Fig.S3). From Fig.1g and 1h, both Pd@Au and Pd@Pt with different ratios have broad near-infrared absorption. While keeping the amount of Pd changeless, the absorption strength of Pd@Au or Pd@Pt increased as the Au/Pd or Pt/Pd mass ratios

increased, and the maximum absorption peak was blue-shifted gradually

**Mimic enzymatic activity of Pd-based nanoplates**

Pd and Pt nanoparticles have been reported to exhibit peroxidase-, oxidase- or catalase-like activity.[16, 18, 22-25, 36] However, there are few studies on the mimetic enzymatic activity of their two-dimensional (2D) nanostructures, especially Pd-based nanoplates. Therefore, we explore the enzyme-like catalytic properties of 2D Pd-based nanostructures including Pd, Pd@Au and Pd@Pt nanoplates. First, the catalytic experiments were carried out using the typical peroxidase substrate 3,3'5,5'-tetramethylbenzidine (TMB) with and without $H_2O_2$ (HAc-NaAc buffer solution, pH 4.5) in the presence of Pd-based nanoplates. The TMB cation free radical, a one-electron oxidation product, would be formed during the reaction procedure, which is responsible for the blue color (maximum absorbance at 652 nm). Time-dependent absorbance changes at 652 nm and absorbance spectra were measured as shown in Fig.2 (a-d). The results showed that the Pd-based nanoplates could catalyze the oxidation of TMB by $H_2O_2$ or dissolved $O_2$ to produce a blue color product (Fig.2b and 2d), suggesting peroxidase-like or oxidase-like activity. Because dissolved $O_2$ is less in the reaction system, the oxidase-like activity of Pd-based nanoplates is lower than their peroxidase-like activity. Moreover, it should be noted that even on the same type of reaction, such as peroxidase-like catalytic reaction, different Pd-based nanoplates demonstrated different activity, and the activity order was: Pd@Pt>Pd>Pd@Au. Meanwhile, we also found that the Pd-based nanoplates could decompose $H_2O_2$ to generate $O_2$ (Fig.2f) in neutral or alkaline condition, showing the catalase-like activity. By measuring the pressure value in a closed system,[52] the catalase-like activity of different catalysts was evaluated in that order: Pd@Pt>Pd>catalase>Pd@Au (Fig.2e). The above results indicate that 2D Pd-based nanoplates possess peroxidase-, oxidase- and catalase-like activities (Fig.S4), but catalytic activities are different with different catalysts.

The enzyme-like catalytic mechanism of noble metal has been reported in related literature.[53] We inferred our Pd-based nanoplates followed similar catalytic mechanisms. In acidic conditions, Pd-based nanoplates acting as peroxidase catalyze $H_2O_2$ decomposition to generate •OH (which had been confirmed in the following section of comparing the peroxidase-like activity of Pd-based nanoplates), resulting in the oxidation of substrates. While in basic conditions, Pd-based nanoplates behave catalase activity to catalyze the conversion of $H_2O_2$ to $H_2O$ and $O_2$. Therefore, Pd-based nanoplates demonstrated different mimetic enzyme activities under different conditions.

Because catalysts with peroxidase activity have a wide range of practical application, and Pd-based nanoplates show excellent catalytic performance in the oxidation of TMB by $H_2O_2$ (Scheme S1), here, we focus the investigation on the peroxidase-like activity of Pd-based nanoplates.

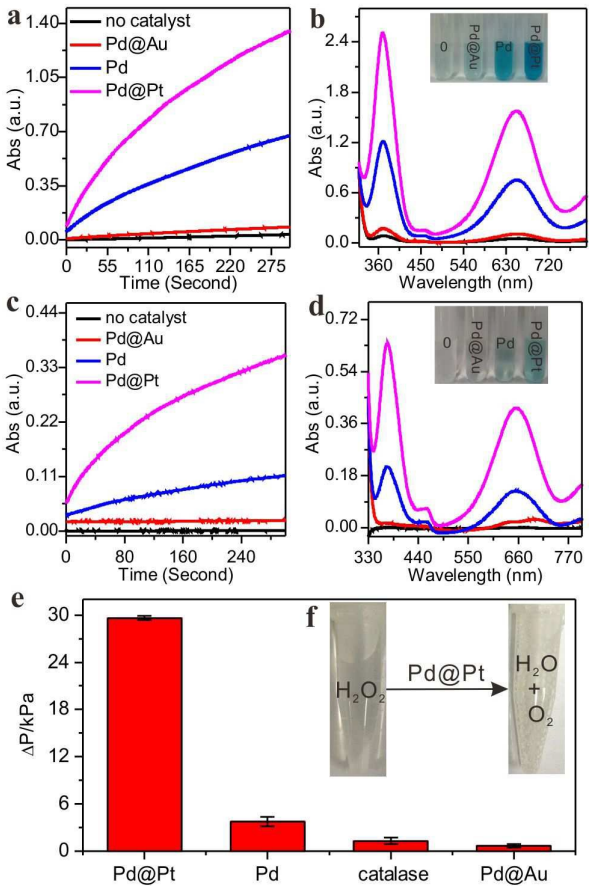


**Fig.2** Mimic enzymatic activity of Pd-based nanoplates. Time-dependent absorbance changes at 652 nm (a) and absorbance spectra (b) of 0.25 mM TMB solutions containing 5 mM $H_2O_2$ without or with Pd@Au, Pd and Pd@Pt nanoplates. Insets show the color change of different samples after 5 min reaction, respectively. Time-dependent absorbance changes at 652 nm (c) and absorbance spectra (d) of 0.5 mM TMB solutions in the absence of $H_2O_2$ without or with Pd@Au, Pd and Pd@Pt nanoplates. Insets show the color change of different samples after 5 min reaction, respectively. (e) The pressure value of generated $O_2$ in a closed system with different catalysts. (f) Pd-based nanoplates as catalase-like catalysts to decompose $H_2O_2$ and generate $O_2$ gas bubbles.

**Experimental condition optimization**

Similar to horseradish peroxidase, the catalytic activity of Pd-based nanoplates is dependent on pH, temperature, $H_2O_2$ concentration and the mass of catalyst. Take Pd@Pt as an example, we measured its peroxidase-like activity by varying the pH from 2 to 12, the temperature from 25°C to 70°C, the $H_2O_2$ concentration from 0 to 0.4 M and the catalysis mass from 0 to 0.65 μg. As shown in Fig.3a, the catalytic activity increased with the increasing pH from 2.0 to 4.9, and then decreased. The optimal pH was approximately 4.5. From Fig.3b, the catalytic activity of Pd@Pt nanoplates remained nearly

unchanged from 25°C to 55°C. Therefore, room temperature was recommended. Fig.3c showed time-dependent absorbance changes (at 652 nm) against different mass of Pd@Pt nanoplates. Dramatic improvement of reaction rate could be observed with the steady increase of the Pd@Pt catalyst. Also, the catalytic activity of Pd@Pt nanoplates gradually increased as the increase of $H_2O_2$ concentration (Fig.S5), but the growth rate became slow under high $H_2O_2$ concentration (Fig.3d). In order to highlight the action of catalysts as well as avoid the self-decomposition of $H_2O_2$ at higher concentration, a $H_2O_2$ concentration of 10 mM was adopted for the following experiments.

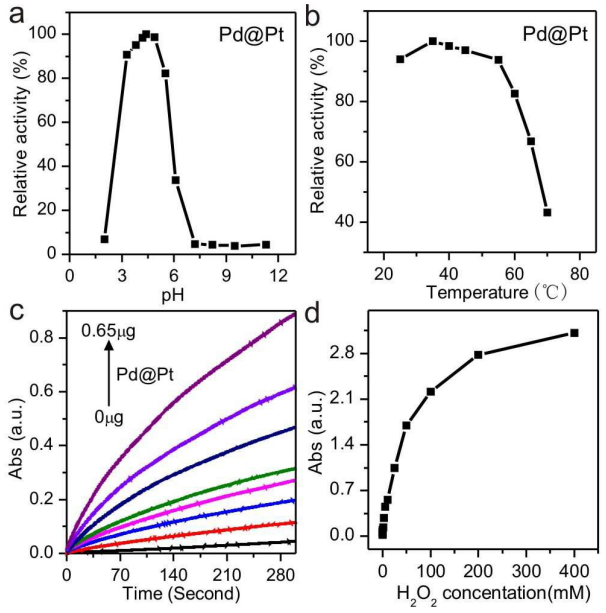


**Fig.3** The peroxidase-like activity of Pd-based nanoplates depends on pH (a), temperature (b), catalyst concentration (c), and $H_2O_2$ concentration (d). (c) Time-dependent absorbance changes at 652 nm with different amounts of Pd@Pt nanoplates. (d) The absorbance values at 652 nm after reaction 5 min with different $H_2O_2$ concentrations.

**Comparing the peroxidase-like activity of Pd-based nanoplates**

As the research moves along, we found that the peroxidase-like activity of Pd-based nanoplates was composition and structure dependent. Fig.4 is the absorbance changes with time and absorbance spectra in the mixture of TMB (0.5 mM) and $H_2O_2$ (10 mM) in the presence of Pd, Pd@Au and Pd@Pt with different ratios (The mass of catalyst in Figure 4a and 4b is ten times higher than that in Fig.4c and 4d). As observed from Fig.4a and 4b, the peroxidase-like activity of Pd@Au is lower than Pd, and the activity decreased gradually with the increasing ratios of Au/Pd from 1.5:1 to 8.2:1. Since Pd is the main contribution for the peroxidase-like activity compared to Au, as the coverage degree of Au on Pd increased, the peroxidase-like activity of Pd@Au became lower and lower. In contrast, Pd@Pt had a higher peroxidase-like activity than Pd. Increasing the Pt/Pd ratios from 1.3:1 to 12:1, a gradual enhancement in activity is observed, indicating Pt nanodots and Pd are together responsible for the oxidation of TMB (Fig.4c and 4d). In addition, the island growth mode of Pt nanodots on Pd also possibly plays an important role for contributing superior peroxidase-like activity compared to Pd@Au nanostructure in which Au was grown epitaxially on the Pd.

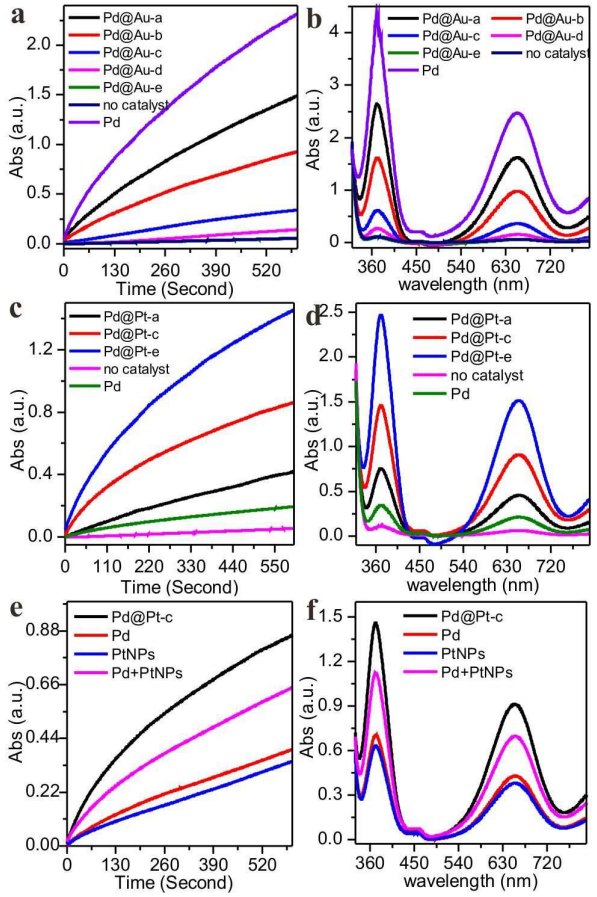


**Fig.4** Time-dependent absorbance changes at 652 nm and absorbance spectra of 0.5 mM TMB solutions containing 10 mM $H_2O_2$ with different ratios of Pd@Au (a and b) or Pd@Pt nanoplates (c and d) (The quality of Pd@Au is ten times that of Pd@Pt nanoplates). (e and f ) The comparison of peroxidase activity of Pd NSs, Pd@Pt nanoplates and Pt NPs. Time-dependent absorbance changes at 652 nm (e) and UV-Vis spectra (f) of 0.5 mM TMB solutions containing 10 mM $H_2O_2$ with different catalysts: Pd@Pt nanoplates, Pd NSs, Pt NPs and physical mixture of Pd NSs and Pt NPs (the amounts of Pd NSs and Pt NPs are same as those in the Pd@Pt nanoplates).

Next, we further investigate if the outstanding peroxidase-like of Pd@Pt nanoplates is due to the strong synergetic effect of Pd and Pt. For comparison, time-dependent absorbance curves under the same condition with Pd, Pt nanoparticles (NPs) or a physical mixture of Pd and Pt NPs as catalysts were

also studied, in which the amounts of Pd and Pt NPs were same as those in the Pd@Pt bimetallic nanoplates. Fig.4e and 4f clearly indicated that the catalytic activity of TMB-$H_2O_2$-Pd@Pt system was the highest, while Pd, Pt NPs alone or the simple mixing of Pd and Pt NPs exhibited less activity towards the oxidation of TMB. In addition, Pd@Pt nanoplates with other ratios also showed similar enhanced catalytic activity (Fig.S6). Previous research had reported that Pt NPs deposited on some supports, like $MoO_3$,[27] $Fe_3O_4$,[28] or formed bimetallic nanostructure and alloy,[22, 25] showed enhanced mimic enzymatic activity due to the synergetic co-catalytic effect of Pt nanocrystals and metal. A similar synergistic effect between Pt nanodots and Pd nanosheets might contribute to the enhanced catalytic activity in the Pd@Pt nanoplates.

As mentioned above, the possible mechanism of peroxidase-like activity of Pd-based nanoplates might originate from their catalytic ability toward the decomposition of $H_2O_2$ in acidic condition to generate hydroxyl radical (•OH). To evidence this assumption, the •OH formation was assessed by adding the fluorescent probe terephthalic acid (TA) into the $H_2O_2$-Pd@Pt system, where terephthalic acid easily reacted with •OH to form highly fluorescent 2-hydroxy terephthalicacid (TAOH), which emitted unique fluorescence around 435 nm.[34, 54] Fig.S7 in Supporting Information showed the fluorescence change in the mixed solution of Pd@Pt, TA, and $H_2O_2$. After 12 h reaction, the remarkable fluorescence enhancement at 435 nm was observed in Pd@Pt-TA-$H_2O_2$ system, while there was no obvious fluorescence change in the absence of $H_2O_2$ or Pd@Pt, suggesting that Pd@Pt could decompose $H_2O_2$ to generate the •OH radical. In addition, the decreased TMB oxidation with time was also observed by the addition of •OH scavenger, DMSO, further indicating the generation of •OH.

Moreover, in order to prove the catalytic activities arising from themselves, the as-prepared Pd@Pt was kept in HAc-NaAc buffer solution (pH 4.5) for 6 h and then catalyzed the oxidation of TMB. Subsequently, Pd@Pt was centrifuged for catalytic reaction again. As shown in the Fig.S8, before and after centrifugation, Pd@Pt showed almost the same catalytic activities. Also we incubated the Pd@Pt nanoplates at temperature range from 4 °C to 90 °C and pH range from 2 to 12 for 2 h, and then measured their peroxidase activities under standard conditions (pH 4.5, room temperature). The Pd@Pt nanoplates were indeed found to remain stable over a wide range of pH from 2 to 12 (Fig.S9a), and temperatures from 4 to 90 °C (Fig.S9b), which are more stable than the natural enzymes like HRP[8] under harsh condition. In addition, after storing Pd@Pt in water for one week, they still remain good catalytic activity (Fig.S10). The experimental results above further confirmed that the catalytic activities originated from the Pd@Pt themselves and the catalyst was stable under harsh condition.

It should be noted that though Pd@Pt themselves demonstrated good thermal stability at high temperature (Fig.S9b), their peroxidase-like activity decreased under higher temperature (Fig.3b). A main reason is due to thermally induced instability of enzymatic product.[55] The TMB cation free radical, a one-electron oxidation product (oxTMB) is unstable at relatively high temperature such as 80℃, which tends to return to thermostable TMB and two-electronic oxidation product (oxfTMB) (demonstrated by the color change and the fast decreasing of UV−Vis signal, Fig.S11).

**Kinetic studies of the peroxidase-like activity of Pd-based nanoplates**

In order to regulate enzyme activity and understand the relationship between nanostructure and enzyme kinetic parameters, the Michaelis–Menten behaviors of Pd@Pt and Pd were studied with $H_2O_2$ and TMB as substrates (Fig.5 and Fig.S12 in supporting information). A series of experiments were carried out by changing the concentration of one substrate and keeping the other constant (Fig.5a and 5b). Typical Michaelis-Menten curves can be obtained for TMB and $H_2O_2$ in a certain concentration range (Fig.5c and 5d). The Michaelis–Menten constant $K_m$ and the maximum initial velocity $V_{max}$ were obtained from the Lineweaver–Burk graphs ($1/V$ versus $1/[S]$) (Fig.5e and 5f, the detailed calculating process was presented in Supporting Information).[56, 57] Km was an indicator of enzyme affinity to substrates. A larger $K_m$ stands for a lower affinity whereas a smaller value indicates a higher affinity. Meanwhile, $K_{cat,}$ one of the most important characterizations to assess the catalytic efficiency of nanomaterials based artificial enzyme, was also calculated and compared with some literature values. The greater value of $K_{cat}$, the higher the enzymatic activity is. The catalytic parameters of Pd@Pt and Pd are summarized in Table 1. The $K_m$ value of Pd@Pt with TMB as the substrate is 1.27 times lower than that of Pd, 5 times lower than that of natural enzyme HRP[8] and 1.13 times lower than that of $Fe_3O_4$ NPs.[8] The $K_m$ value of Pd@Pt with $H_2O_2$ as the substrate is 1.97 times lower than that of Pd, 1.66 times lower than that of HRP and 69 times lower than that of $Fe_3O_4$ NPs. The $K_{cat}$ of Pd@Pt and Pd nanoplates with TMB and $H_2O_2$ as substrates are larger than that of HRP and comparable with $Fe_3O_4$ MNPs. These results indicated that 2D bimetallic Pd@Pt had a high binding affinity towards TMB and $H_2O_2$, and could be applied to detect $H_2O_2$ through colorimetric or electrochemical method.

**Table 1** Comparison of the kinetic parameters of different catalysts. [E] is the catalyst concentration, $K_m$ is the Michaelis constant, $V_{max}$ is the maximal reaction velocity and $K_{cat}$ is the catalytic constant, where $K_{cat}=V_{max}/[E]$.

| Catalysts | [E] (M) | Substrate | $K_m$(mM) | $V_{max}$(M $s^{-1}$) | $K_{cat}$($s^{-1}$) |
|---|---|---|---|---|---|
| Pd@Pt | $1.9\times10^{-12}$ | TMB | 0.0865 | $6.228\times10^{-8}$ | $3.1\times10^{4}$ |
| | | $H_2O_2$ | 2.231 | $5\times10^{-8}$ | $2.5\times10^{4}$ |
| Pd | $5.06\times10^{-12}$ | TMB | 0.1098 | $5.82\times10^{-8}$ | $1.2\times10^{4}$ |
| | | $H_2O_2$ | 4.398 | $6.51\times10^{-8}$ | $1.3\times10^{4}$ |
| HRP[8] | $2.5\times10^{-11}$ | TMB | 0.434 | $10\times10^{-8}$ | $4\times10^{3}$ |
| | | $H_2O_2$ | 3.7 | $8.71\times10^{-8}$ | $3.48\times10^{3}$ |
| $Fe_3O_4$MNPs[8] | $11.4\times10^{-13}$ | TMB | 0.098 | $3.44\times10^{-8}$ | $3.02\times10^{4}$ |
| | | $H_2O_2$ | 154 | $9.78\times10^{-8}$ | $8.58\times10^{4}$ |

For further investigating the catalytic mechanism of Pd@Pt nanoplates, we measured their catalytic activity over a range of TMB and $H_2O_2$ concentrations. As shown in Fig. S13, double

reciprocal plots of initial velocity versus one substrate concentration were obtained for a range of concentrations of the second substrate (Fig.S13c and S13d). The slopes of the lines are parallel, which is characteristic of a ping-pong mechanism, as is observed for HRP[58] and some mimetic peroxidases like $Fe_3O_4$[8] and GO-COOH.[12] These results showed that, similar to HRP, the Pd@Pt bind and react with the first substrate, releasing the first product before reacting with the second substrate.

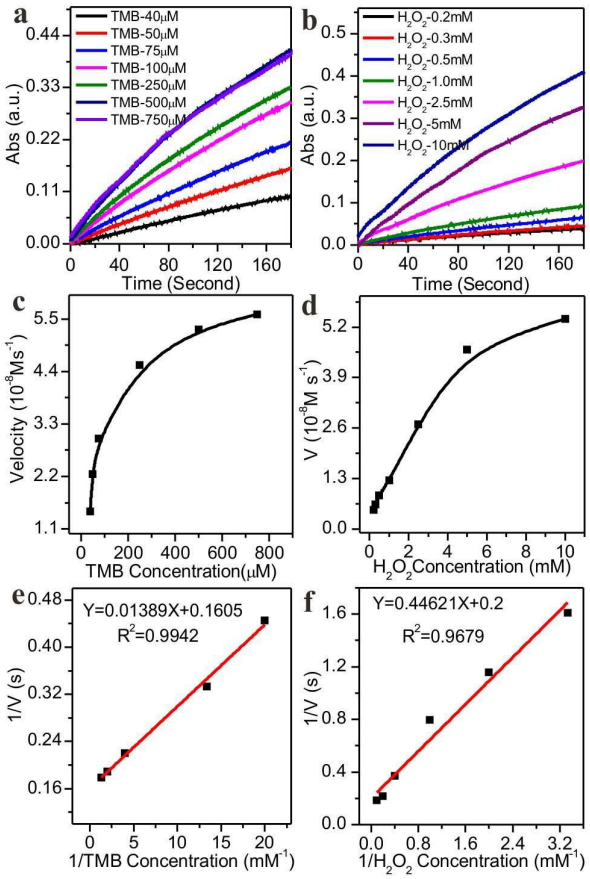


**Fig.5** Steady-state kinetic assay of Pd@Pt-c. Time-dependent absorbance changes at 652 nm of TMB reaction solutions catalyzed by the Pd@Pt-c in the presence of different concentrations of TMB (a) or $H_2O_2$ (b). The velocity (v) of the reaction changes in the presence of different concentrations of TMB (c) or $H_2O_2$ (d). Double reciprocal plots of activity of Pd@Pt-c in the presence of different concentrations of TMB (e) or $H_2O_2$ (f), respectively. Experiments were carried out in acetic acid-sodium acetate buffer (pH 4.5) using 0.2 μg Pd@Pt-c at 25℃. (a), (c) and (e) $H_2O_2$ concentration was fixed at 10 mM and the TMB concentration was varied. (b), (d) and (f) TMB concentration was fixed at 0.5 mM and the $H_2O_2$ concentration was varied.

**Colorimetric detection of $H_2O_2$ and glucose**

As demonstrated above, the absorbance changes of TMB oxidation catalyzed by Pd@Pt is $H_2O_2$ concentration-dependent and can be used for $H_2O_2$ detection. Fig.6a shows typical $H_2O_2$ concentration response curve under optimal conditions. There is a good linear relationship between the absorbance of TMB at 652 nm and the concentration of $H_2O_2$ in the range of 0.004-2 mM with a detection limit of 4 μM (Fig.6b). Since $H_2O_2$ is the main by-product of the glucose oxidase (GOx)-catalyzed reaction, colorimetric detection of glucose can also be realized through combining peroxidase-like activity of Pd@Pt and specific catalytic oxidation of glucose by GOx (The detailed procedure is described in the Experimental Section). Fig.6c shows a typical glucose concentration response curve, and glucose can be detected in the linear range from 0.1 mM to 0.5 mM.

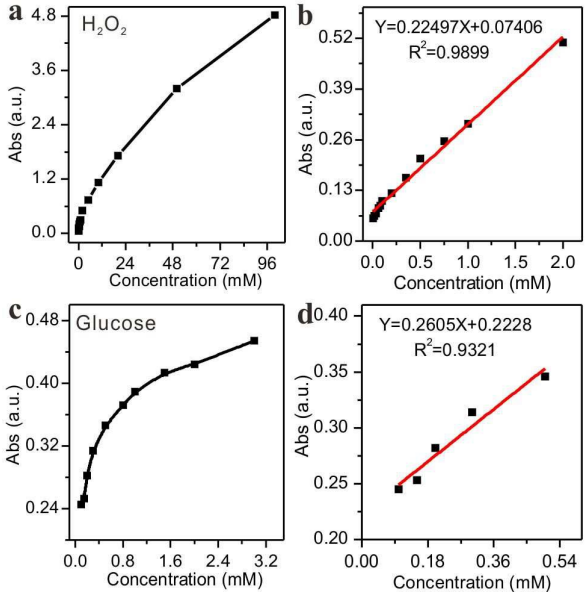


**Fig.6** A dose–response curve for (a) $H_2O_2$, (c) glucose detection at 652 nm under the optimum conditions. (b) and (d) show their respective linear calibration plots.

**Electrochemical $H_2O_2$ analysis**

Fig.7 shows the electrochemical responses to $H_2O_2$ of various concentrations using the Pd, Pd@Pt or Pd@Au modified electrodes. These Pd-based nanoplates all manifest the voltammetric characteristics with direct responses to successive additions of $H_2O_2$, where the $H_2O_2$ reduction currents can increase proportionally with $H_2O_2$ levels. Typical current–time responses of Pd, Pd@Pt or Pd@Au modified electrodes to $H_2O_2$ were compared in the Fig.7d. Similar to the results of colorimetric reaction, Pd@Pt and Pd behaved excellent electrochemical activity compare with the Pd@Au, due to their different constitutes and structures mentioned above. Here, we only simply compared the electrochemical activity of 2D Pd-based nanoplates to $H_2O_2$ responses. Detailed electrochemical sensing applications of these 2D Pd-based nanoplates are under investigating.

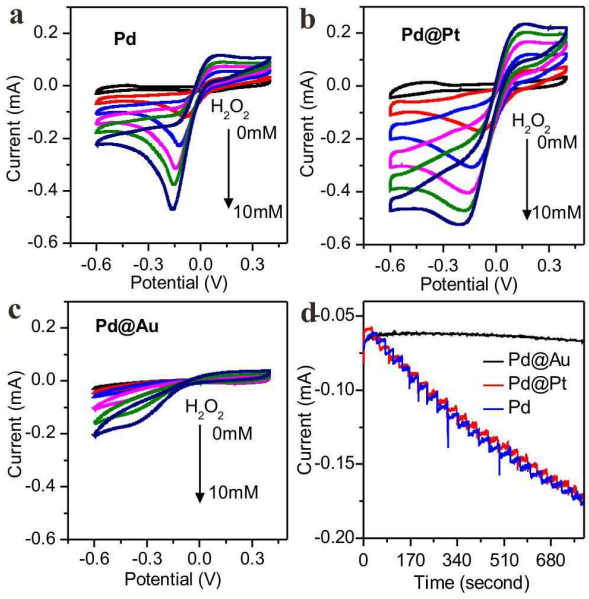


**Fig.7** Direct electrochemical response to $H_2O_2$. Cyclic voltammograms responses of different metallic catalysts (a) Pd, (b) Pd@Pt and (c) Pd@Au modified electrodes to the increase of $H_2O_2$ concentrations from 0 to 10 mM with a step of 2 mM in PBS (pH = 7.4), at 50 mV $s^{-1}$ scan rate. (d) The amperometric response curves of the Pd, Pd@Pt and Pd@Au modified electrodes toward the $H_2O_2$ with a step of 0.1 mM $H_2O_2$ at an applied potential of -0.2 V in PBS (pH = 7.4), at 50 mV $s^{-1}$ scan rate.

## Conclusion

In summary, our studies indicate that 2D Pd-based nanostructures (Pd, Pd@Au and Pd@Pt) possess intrinstic peroxidase-, oxidase- and catalase-like activity and the catalytic activities are structure- and composition- dependent. Of them, Pd@Pt demonstrates a superior catalytic activity in TMB oxidation over its monometallic counterpart alone or the physical mixture of two monometallic components. The excellently catalytic performance could be attributed to the synergistic interaction of two components. Kinetic analysis also indicates that the catalytic activity of Pd@Pt was comparable to other reported catalysts. With the advantages of low cost, easy preparation, good stability, and tunable composition and structure, these Pd-based nanostructures have the potentials as a promising enzyme mimetic candidate and may find wide applications in biocatalysis, bioassays, and nano-biomedicine

## Acknowledgements

The work was financially supported by the National Natural Science Foundation of China (No.21101131, 221420102001, 21131005), National Basic Research Foundation (973) of China (2014CB932004, 2011CB932403), Natural Science Foundation of Fujian Province (No.2012J01056), Fundamental Research Funds for the Central Universities (2010121015), and the open project grant from State Key Laboratory of Chemo/biosensing and Chemometrics (2013009). We thank Fang Liu and Dan Liu in Professor Chaoyong Yang group for help the measurement of catalase-like activities.

## Notes and references

1. Y. L. Dong, H. G. Zhang, Z. U. Rahman, L. Su, X. J. Chen, J. Hu and X. G. Chen, *Nanoscale*, 2012, **4**, 3969-3976.
2. Y. Lin, J. Ren and X. Qu, *Acc. Chem. Res.*, 2014, **47**, 1097-1105.
3. M. J. Wiester, P. A. Ulmann and C. A. Mirkin, *Angew. Chem. Int. Ed.*, 2011, **50**, 114-137.
4. X. Chen, H. Yang, Q. Zhu, H. Zheng, J. Xu and D. Li, *Analyst*, 2001, **126**, 523-527.
5. Q. Wang, Z. Yang, X. Zhang, X. Xiao, C. K. Chang and B. Xu, *Angew. Chem. Int. Ed.*, 2007, **46**, 4285-4289.
6. L. Fruk and C. M. Niemeyer, *Angew. Chem. Int. Ed.*, 2005, **44**, 2603-2606.
7. L. Ai, L. Li, C. Zhang, J. Fu and J. Jiang, *Chem. Eur. J.*, 2013, **19**, 15105-15108.
8. L. Gao, J. Zhuang, L. Nie, J. Zhang, Y. Zhang, N. Gu, T. Wang, J. Feng, D. Yang, S. Perrett and X. Yan, *Nat. Nanotechnol.*, 2007, **2**, 577-583.
9. H. Wei and E. Wang, *Anal. Chem.*, 2008, **80**, 2250-2254.
10. Z. Dai, S. Liu, J. Bao and H. Ju, *Chem. Eur. J.*, 2009, **15**, 4321-4326.
11. Y. Song, X. Wang, C. Zhao, K. Qu, J. Ren and X. Qu, *Chem. Eur. J.*, 2010, **16**, 3617-3621.
12. Y. Song, K. Qu, C. Zhao, J. Ren and X. Qu, *Adv. Mater.*, 2010, **22**, 2206-2210.
13. A. Asati, S. Santra, C. Kaittanis, S. Nath and J. M. Perez, *Angew. Chem. Int. Ed.*, 2009, **48**, 2308-2312.
14. Y. Chen, H. Cao, W. Shi, H. Liu and Y. Huang, *Chem. Commun.*, 2013, **49**, 5013-5015.
15. A. K. Dutta, S. Das, S. Samanta, P. K. Samanta, B. Adhikary and P. Biswas, *Talanta*, 2013, **107**, 361-367.
16. J. Fan, J. J. Yin, B. Ning, X. Wu, Y. Hu, M. Ferrari, G. J. Anderson, J. Wei, Y. Zhao and G. Nie, *Biomaterials*, 2011, **32**, 1611-1618.
17. T. Hamasaki, T. Kashiwagi, T. Imada, N. Nakamichi, S. Aramaki, K. Toh, S. Morisawa, H. Shimakoshi, Y. Hisaeda and S. Shirahata, *Langmuir*, 2008, **24**, 7354-7364.
18. Z. Gao, M. Xu, L. Hou, G. Chen and D. Tang, *Anal. Chim. Acta.*, 2013, **776**, 79-86.
19. Y. Jv, B. Li and R. Cao, *Chem. Commun.*, 2010, **46**, 8017-8019.
20. X. X. Wang, Q. Wu, Z. Shan and Q. M. Huang, *Biosensors and Bioelectronics*, 2011, **26**, 3614-3619.
21. W. J. Luo, C. F. Zhu, S. Su, D Li, Y. He, Q. Huang and C. H. Fan, *ACS Nano*, 2010, **4**, 7451-7458.
22. W. He, X. Wu, J. Liu, X. Hu, K. Zhang, S. Hou, W. Zhou and S. Xie, *Chem. Mater.*, 2010, **22**, 2988-2994.
23. J. Liu, X. Hu, S. Hou, T. Wen, W. Liu, X. Zhu, J.-J. Yin and X. Wu, *Sensors and Actuators B*, 2012, **166-167**, 708-714.

24. W. He, Y. Liu, J. Yuan, J. J. Yin, X. Wu, X. Hu, K. Zhang, J. Liu, C. Chen, Y. Ji and Y. Guo, *Biomaterials*, 2011, **32**, 1139-1147.
25. K. Zhang, X. Hu, J. Liu, J. J. Yin, S. Hou, T. Wen, W. He, Y. Ji, Y. Guo, Q. Wang and X. Wu, *Langmuir*, 2011, **27**, 2796-2803.
26. Y. Tao, Y. Lin, Z. Huang, J. Ren and X. Qu, *Adv. Mater.*, 2013, **25**, 2594-2599.
27. Y. Wang, X. Zhang, Z. Luo, X. Huang, C. Tan, H. Li, B. Zheng, B. Li, Y. Huang, J. Yang, Y. Zong, Y. Ying and H. Zhang, *Nanoscale*, 2014, **6**, 12340-12344.
28. M. Ma, J. Xie, Y. Zhang, Z. Chen and N. Gu, *Mater. Lett.*, 2013, **105**, 36-39.
29. H. Wang, S. Li, Y. Si, N. Zhang, Z. Sun, H. Wu and Y. Lin, *Nanoscale*, 2014, **6**, 8107.
30. H. Chen, Y. Li, F. Zhang, G. Zhang and X. Fan, *J. Mater. Chem.*, 2011, **21**, 17658.
31. X. Zhang, G. Wu, Z. Cai and X. Chen, *Talanta*, 2015, **134**, 132-135.
32. Y. Lin, Z. Li, Z. Chen, J. Ren and X. Qu, *Biomaterials*, 2013, **34**, 2600-2610.
33. Z. Wang, X. Yang, J. Yang, Y. Jiang and N. He, *Anal. Chim. Acta.*, 2015, **862**, 53-63.
34. Y. Tao, E. Ju, J. Ren and X. Qu, *Adv. Mater.*, 2015, **27**, 1097-1104.
35. Y. Nangia, B. Kumar, J. Kaushal and C. R. Suri, *Anal. Chim. Acta.*, 2012, **751**, 140-145.
36. Z. Zhu, Z. Guan, S. Jia, Z. Lei, S. Lin, H. Zhang, Y. Ma, Z. Q. Tian and C. J. Yang, *Angew. Chem. Int. Ed.*, 2014, **53**, 12503-12507.
37. X. Lv and J. Weng, *Scientific reports*, 2013, **3**, 3285.
38. S. Eustis and M. A. El. Sayed, *Chem.Soc.Rev.*, 2006, **35**, 209–217.
39. S. E. Skrabalak, J. Chen, Y. Sun, X. Lu, L. Au, C. M. Cobley and Y. Xia, *Acc. Chem. Res.*, 2008, **41**, 1587-1595.
40. J. N. Anker, W. P. Hall, O. Lyandres, N. C. Shah, J. Zhao and R. P. Van Duyne, *Nat. Mater.,* 2008, **7**, 442-453.
41. X. Huang, S. Tang, X. Mu, Y. Dai, G. Chen, Z. Zhou, F. Ruan, Z. Yang and N. Zheng, *Nat. Nanotechnol.*, 2011, **6**, 28-32.
42. L. Nie, M. Chen, X. Sun, P. Rong, N. Zheng and X. Chen, *Nanoscale*, 2014, **6**, 1271-1276.
43. S. Tang, M. Chen and N. Zheng, *Small*, 2014, **10**, 3139-3144.
44. Z. Zhao, S. Shi, Y. Huang, S. Tang and X. Chen, *ACS Appl. Mater. Interfaces*, 2014, **6**, 8878-8885.
45. S. H. Tang, M. Chen and N. F. Zheng, *Nano Research*, 2015, **8**, 165-174.
46. Y. Dai, S. Liu and N. Zheng, *J. Am. Chem. Soc.*, 2014, **136**, 5583-5586.
47. X. Huang, S. Tang, B. Liu, B. Ren and N. Zheng, *Adv. Mater.*, 2011, **23**, 3420-3425.
48. M. Chen, B. Wu, J. Yang and N. Zheng, *Adv. Mater.*, 2012, **24**, 862-879.
49. X. Wang, B. Wu, G. Chen, Y. Zhao, P. Liu, Y. Dai and N. Zheng, *Nanoscale*, 2014, **6**, 6798-6804.
50. M. Chen, S. Tang, Z. Guo, X. Wang, S. Mo, X. Huang, G. Liu and N. Zheng, *Adv. Mater.*, 2014, **26**, 8210-8216.
51. S. Mo, X. Chen, M. Chen, C. He, Y. Lu and N. Zheng, *J. Mater. Chem. B*, 2015, **3**, 6255-6260.
52. Z. Zhu, Z. Guan, D. Liu, S. Jia, J. Li, Z. Lei, S. Lin, T. Ji, Z. Tian and C. J. Yang, *Angew. Chem. Int. Ed.*, 2015, **54**,1-6.
53. J. Li, W. Liu, X. Wu and X. Gao, *Biomaterials*, 2015, **48**, 37-44.
54. K. Ishibashia, A. Fujishima, T. Watanabe, K. Hashimoto, Journal of Photochemistry and Photobiology A, 2000, **134**,139-142
55. Y. Lin, A. Zhao, Y. Tao, J. Ren and X. Qu, *J. Am. Chem. Soc.*, 2013, **135**, 4207-4210.
56. L. A. Marquez and H. B. Dunford, *Biochemistry*, 1997, **36**, 9349-9355.
57. P. D. Josephy, T. Eling and R. P. Mason, *J. Biol. Chem.*, 1982, **257**, 3669-3675.
58. D. J. T. Porter and H. J. Brights, *J. Biol. Chem.*, 1983, **258**, 9913-9924.

## TOC graphics

2D Pd-based nanostructures possess intrinstic peroxidase-, oxidase- and catalase-like activity and the catalytic activities are structure- and composition- dependent.